

Are the Kepler Near-Resonance Planet Pairs due to Tidal Dissipation?

Man Hoi Lee¹, D. Fabrycky^{2,3,4}, and D. N. C. Lin^{3,5}

¹ *Department of Earth Sciences and Department of Physics, The University of Hong Kong, Pokfulam Road, Hong Kong*

² *Department of Astronomy and Astrophysics, University of Chicago, 5640 S. Ellis Ave., Chicago, IL 60637, USA*

³ *UCO/Lick Observatory, University of California, Santa Cruz, CA 95064, USA*

⁴ *Hubble Fellow*

⁵ *Kavli Institute for Astronomy and Astrophysics and School of Physics, Peking University, China*

ABSTRACT

The multiple-planet systems discovered by the Kepler mission show an excess of planet pairs with period ratios just wide of exact commensurability for first-order resonances like 2:1 and 3:2. In principle, these planet pairs could have both resonance angles associated with the resonance librating if the orbital eccentricities are sufficiently small, because the width of first-order resonances diverges in the limit of vanishingly small eccentricity. We consider a widely-held scenario in which pairs of planets were captured into first-order resonances by migration due to planet-disk interactions, and subsequently became detached from the resonances, due to tidal dissipation in the planets. In the context of this scenario, we find a constraint on the ratio of the planet's tidal dissipation function and Love number that implies that some of the Kepler planets are likely solid. However, tides are not strong enough to move many of the planet pairs to the observed separations, suggesting that additional dissipative processes are at play.

1. INTRODUCTION

The *Kepler* space telescope is designed to detect the periodic transits of exoplanets in front of their host stars. Based on the data obtained during the first 16 months of Kepler's operation, more than 2000 planetary candidates have been identified, analyzed, and published (Batalha et al. 2013). Most of these planetary candidates have radii in the range 1–4 times that of the Earth (R_{\oplus}) and orbital periods P less than a few months. The rarity of planets with smaller radii and longer periods is due to observational selection effects. Although a large fraction of these candidates may indeed be planets, some of them may be due to the blending of background eclipsing binary stars with the light of foreground stars.

In the 16-month Kepler catalog¹, there are 361 host stars which bear two or more transiting planetary candidates (Fabrycky et al. 2012), and almost all of them are real multiple-planet systems (Lissauer et al. 2012). Their orbital configurations contain valuable information on the history of their formation and dynamical evolution. In particular, although a majority of the planet pairs are not in or near mean-motion resonances, there is an excess of planet pairs with outer-to-inner orbital period ratios, P_2/P_1 , just wide of first-order 2:1 and 3:2 resonances and a deficit of pairs with P_2/P_1 just smaller than 2:1 and 3:2 (Lissauer et al. 2011; Fabrycky et al. 2012). The excess and deficit occur within a few percent of exact commensurabilities. Figure 1 shows the histogram of period ratio for all Kepler candidate pairs, pairs with radius of the inner planet $R_1 < 2R_\oplus$ (Earths and super-Earths), and pairs with $R_1 > 2R_\oplus$ (Neptunes and above). Both pairs with $R_1 < 2R_\oplus$, and pairs with $R_1 > 2R_\oplus$ show an excess for P_2/P_1 just larger than 3:2 and a deficit just smaller than 2:1, but interestingly, there is not an obvious excess just larger than 2:1 for pairs with $R_1 < 2R_\oplus$ (although the statistics is noisy due to small numbers). Also, the lack of pairs with P_2/P_1 just smaller than 3:2 reported by Fabrycky et al. (2012) is not noticeable in Figure 1, because the bin size (0.05) is large compared to the width of the gap (0.01–0.02).²

The Kepler candidates should be contrasted with the radial velocity sample, which also shows an excess of planet pairs near the 2:1 resonance. The radial-velocity planets are mostly Jupiter-mass planets, and the excess near the 2:1 resonance consists of confirmed (or likely) resonant pairs such as GJ 876 (Laughlin & Chambers 2001; Rivera & Lissauer 2001; Laughlin et al. 2005) and HD 82943 (Lee et al. 2006; Tan et al. 2013). A widely accepted hypothesis for the origin of such resonances is resonance capture through convergent migration of the planets (Bryden et al. 2000; Kley 2000; Lee & Peale 2002). Tidal interaction between an embedded planet and its natal protoplanetary disk generally leads to a torque imbalance (Goldreich & Tremaine 1980). Jupiter-mass planets are able to open gaps in the disks, and they generally evolve with the viscous diffusion of their natal disks and undergo inward type II migration (except in the outermost regions of the disk where the disk spreads viscously outward and the migration is outward) (Lin & Papaloizou 1986). Convergent migration occurs if the inward migration of the outer planet proceeds faster than that of the inner planet and the outer-to-inner period ratio, P_2/P_1 , decreases.

Lower-mass planets, like most of the Kepler candidates, do not significantly perturb the disk surface density distribution, and thus they undergo type I migration. The direction of type I migration is expected to be inward in the classic theory of, e.g., Ward (1997), but more recent analysis have shown that type I migration could be outward in the viscously heated regions of some

¹ We did not use the 2-year catalog of Burke et al. (2013), which is available at <http://exoplanetarchive.ipac.caltech.edu/>, in this paper, as the 2-year catalog was still changing, with evolving biases and completeness, when we completed this work.

² Fabrycky et al. (2012) have found that the distribution of period ratios around second-order resonances is consistent with a random distribution. The excess of pairs with $R_1 < 2R_\oplus$ (as well as all pairs) for the bin in Figure 1 centered at $P_2/P_1 = 1.725$, which is just wide of the second-order 5:3 resonance, is likely an artifact, as there are no longer obvious features around 5:3 when we shift the bins by, e.g., 0.02 in P_2/P_1 .

disk models (Paardekooper et al. 2011; Kretke & Lin 2012).

Tidal interactions also occur between planets and their host stars, which generally lead toward a state of spin synchronization and orbital circularization (see, e.g., Hut 1981; Peale 1999). If the host spins with a frequency faster (slower) than its companion’s orbital mean motion, the dissipation of the tides raised by the companion in the host would reduce (increase) the host’s spin frequency and increase (decrease) the companion’s orbital semimajor axis on a timescale which is determined by the host’s Q/k_2 value, where Q is the tidal dissipation function and k_2 is the Love number. The companion’s eccentricity is generally damped by the dissipation of the tides raised by the host in the companion on a timescale which is determined by the companion’s Q/k_2 value.

In this paper, we consider in detail a scenario which may account for the Kepler near-resonance planet pairs. Pairs of planets were captured into first-order resonances by convergent migration due to planet-disk interactions, and subsequently became detached from the resonances due to tidal dissipation in the planets. The latter process was proposed by Novak et al. (2003) and more recently by Papaloizou & Terquem (2010), Lithwick & Wu (2012), and Batygin & Morbidelli (2013). In Section 2, we give a simple explanation why the period ratio P_2/P_1 should in fact be slightly larger than the exact period ratio for a first-order resonance, if both resonance angles are librating. We then show that classic type I migration should result in resonant pairs with P_2/P_1 much closer to exact commensurability than the few percent departures observed for the Kepler near-resonance pairs. Subsequent tidal damping of eccentricity and evolution away from exact commensurability are discussed in Section 3, along with known constraints on Q/k_2 for rocky and giant planets. Comparisons with the observed Kepler near-resonance pairs are used to derive constraints on Q/k_2 and the rocky/giant nature of the Kepler planets in Section 4. The results are summarized and discussed in Section 5.

2. RESONANT PLANET PAIRS

For first-order, $j:(j - 1)$, mean-motion resonances like 2:1 and 3:2, there are two eccentricity-type resonance angles,

$$\theta_1 = (j - 1)\lambda_1 - j\lambda_2 + \varpi_1, \tag{1}$$

$$\theta_2 = (j - 1)\lambda_1 - j\lambda_2 + \varpi_2, \tag{2}$$

where λ_i is the mean longitude of planet i and ϖ_i is the longitude of periaapse ($i = 1$ and 2 for the inner and outer planets, respectively). At least one of these angles must librate about a fixed value for the pair to be in resonance, if we ignore inclination resonances. The resonance induced periaapse precession is usually *retrograde*, i.e., $\dot{\varpi}_i < 0$ (see below). In the best example of a mean-motion resonance in extrasolar planetary systems, the 2:1 resonance in GJ 876, both angles librate about 0° , and the periaapses are observed to precess at an average rate of $\dot{\varpi}_i = -41^\circ \text{ yr}^{-1}$ (Laughlin & Chambers 2001; Rivera & Lissauer 2001; Lee & Peale 2002; Laughlin et al. 2005). If

the resonance angle θ_i is librating,

$$\dot{\theta}_i = (j-1)n_1 - jn_2 + \dot{\varpi}_i = 0 \quad (3)$$

on average, or

$$\frac{P_2}{P_1} - \frac{j}{(j-1)} = -\frac{\dot{\varpi}_i}{(j-1)n_2} > 0, \quad (4)$$

where n_i is the mean motion, $P_i = 2\pi/n_i$ is the orbital period, and $\dot{\varpi}_i < 0$ due to the resonance. So P_2/P_1 should in fact be slightly larger than the exact period ratio for a resonant pair.

In the vicinity of a $j:(j-1)$ resonance, the Hamiltonian to the lowest order in the orbital eccentricities e_i is

$$H = -\frac{GM_*M_1}{2a_1} - \frac{GM_*M_2}{2a_2} - \frac{GM_1M_2}{a_2}(C_1e_1 \cos \theta_1 + C_2e_2 \cos \theta_2), \quad (5)$$

where M_* is the stellar mass, M_i is the planetary mass, and a_i is the orbital semimajor axis (e.g., Peale 1986; Murray & Dermott 1999). The coefficients $C_1 = (1/2)(-2j - \alpha D)b_{1/2}^{(j)}$ and $C_2 = (1/2)(-1+2j+\alpha D)b_{1/2}^{(j-1)} - \delta_{j2}/(2\alpha^2)$, where $\alpha = a_1/a_2$, $b_{1/2}^{(j)}(\alpha)$ is the Laplace coefficient, $D = d/d\alpha$, and δ_{j2} is the Kronecker delta. For 2:1, $C_1 = -1.190$ and $C_2 = 0.428$. For 3:2, $C_1 = -2.025$ and $C_2 = 2.444$. The first two terms of the Hamiltonian are the unperturbed Keplerian Hamiltonian and the remaining terms are the resonant interactions. The equation for the variation of the periapse longitude is

$$\frac{d\varpi_i}{dt} = -\frac{\sqrt{1-e_i^2}}{M_i e_i \sqrt{GM_* a_i}} \frac{\partial H}{\partial e_j}, \quad (6)$$

if we assume coplanar orbits. Since libration of θ_1 about 0° and θ_2 about 180° is the only stable resonance configuration for small eccentricities (e.g., Peale 1986; Murray & Dermott 1999; Lee 2004), $\dot{\varpi}_1 = \alpha n_1 (M_2/M_*) C_1/e_1$ and $\dot{\varpi}_2 = -n_2 (M_1/M_*) C_2/e_2$ to the lowest order in eccentricities. Thus $\dot{\varpi}_i \propto -1/e_i$ and $P_2/P_1 - j/(j-1)$ could be large and positive, if the eccentricities are small. This is different from higher-order resonances. For example, for a second-order resonance, the resonant terms in the Hamiltonian to the lowest order in the eccentricities are proportional to e_1^2 , $e_1 e_2$, and e_2^2 , and $\dot{\varpi}_1$ involves terms that are either independent of the eccentricities or proportional to e_2/e_1 (similarly, e_1/e_2 for $\dot{\varpi}_2$).

We can derive two simple relationships between the eccentricities and the period ratio from the above expressions for $\dot{\varpi}_1$ and $\dot{\varpi}_2$. From the requirement that both orbits precess at the same rate on average, i.e., $\dot{\varpi}_1 = \dot{\varpi}_2$,

$$\frac{e_2}{e_1} = -\alpha^{1/2} \frac{C_2 M_1}{C_1 M_2} \quad (7)$$

(Lee 2004). Substituting $\dot{\varpi}_1$ into equation (4),

$$\frac{P_2}{P_1} - \frac{j}{j-1} = \frac{-1}{(j-1)} \alpha^{-1/2} \frac{M_2 C_1}{M_* e_1}. \quad (8)$$

In the above equations, $\alpha = a_1/a_2 \approx [(j-1)/j]^{2/3}$.

Convergent migration of planets due to interactions with the protoplanetary disk can result in capture into mean-motion resonances. This is the most likely scenario for the origin of the 2:1 resonance in the GJ 876 system (Lee & Peale 2002). If the growth of eccentricity due to continued migration within the resonance is balanced by the damping of eccentricity by planet-disk interactions, the eccentricities would reach equilibrium values determined by the ratio of the rates of eccentricity damping and migration. A natural question arises as to whether the Kepler near-resonance pairs are simply resonance pairs with very small eccentricities (and hence large positive departure of P_2/P_1 from exact commensurability) due to large eccentricity damping during disk-induced migration.³ Most of the Kepler candidate planets are sufficiently small that they are unable to open gaps in the protoplanetary disks and should undergo type I migration. For *classic* type I migration, the migration rate is (Ward 1997; Tanaka et al. 2002)

$$\frac{\dot{a}}{a} = -C_a \frac{M_p}{M_*} \frac{\Sigma a^2}{M_*} \left(\frac{H}{a}\right)^{-2} \frac{2\pi}{P}, \quad (9)$$

and the eccentricity damping rate is (Artymowicz 1993)

$$\frac{\dot{e}}{e} = -9C_e \frac{M_p}{M_*} \frac{\Sigma a^2}{M_*} \left(\frac{H}{a}\right)^{-4} \frac{2\pi}{P}, \quad (10)$$

where $C_a \approx 3$, $C_e \approx 0.1$, M_p is the planetary mass, Σ is the surface mass density of the disk, and H/a is the dimensionless scale height of the disk. The ratio

$$K_e = \left| \frac{\dot{e}/e}{\dot{a}/a} \right| = \frac{9C_e}{C_a} \left(\frac{H}{a}\right)^{-2}. \quad (11)$$

For $H/a = 0.05$ and 0.1 , $K_e = 120$ and 30 , respectively.

We have performed direct numerical orbit integrations using the symplectic integrator SyMBA modified to include forced migration and eccentricity damping (Lee & Peale 2002; Lee 2004). Figure 2 shows a convergent migration calculation with $M_* = 1M_\odot$ and $M_1 = M_2 = 10M_\oplus$. The planets are initially far from the 2:1 mean-motion commensurability, and the outer planet is forced to migrate inward with $\dot{a}_2/a_2 \propto P_2^{-1}$ and $K_e = 100$. The pair is captured into 2:1 resonance with both θ_1 and θ_2 librating. The centers of libration change from $\theta_1 = 0^\circ$ and $\theta_2 = 180^\circ$ at small eccentricities to close to $\theta_1 = \theta_2 = 0^\circ$ at large eccentricities (with the offsets from 0° due to the forced migration and eccentricity damping). The eccentricities reach equilibrium values that are too large ($e_1 \approx 0.2$), and P_2/P_1 departs from 2 by less than 0.001 at the end. This result is representative of calculations with $K_e \sim 100$ for both 2:1 and 3:2. Hence the Kepler near-resonance pairs are *not* the result of eccentricity damping within the expected range during disk-induced classic type I migration.

³ At sufficiently small eccentricities, the regions of libration and circulation of the resonant angles are not separated by separatrices, and it is often said that the pair is no longer in resonance (e.g., Delisle et al. 2012). However, our analysis applies as long as the interactions between the planets are dominated by the libration of the resonant angles.

3. TIDAL DAMPING OF ECCENTRICITY

It has been proposed that the subsequent damping of orbital eccentricities by tidal dissipation in the planets may reduce the eccentricities to sufficiently small values to explain the observed departures from exact commensurabilities (Lithwick & Wu 2012; Batygin & Morbidelli 2013). Tidal dissipation in the planet damps the orbital eccentricity on timescale

$$\tau_e = \frac{e}{\dot{e}} = \frac{1}{21\pi} \frac{Q}{k_2} \frac{M_p}{M_*} \left(\frac{a}{R_p} \right)^5 P, \quad (12)$$

while conserving the total angular momentum of the system, where R_p , Q , and k_2 are the radius, tidal dissipation function, and Love number of the planet of mass M_p . The above equation assumes that the planet is synchronously rotating and that Q is constant as a function of the tidal frequencies. Since \dot{e}/e is independent of e and a changes only slightly for small e , one would expect e to decay exponentially. However, as we now demonstrate, the eccentricities do *not* decay exponentially for near-resonance pairs due to interactions between the planets: they decay slowly according to a shallow power law.

Using migration calculations with eccentricity damping similar to that shown in Figure 2, we have assembled several 2:1 and 3:2 configurations with $M_* = 1M_\odot$ and different M_1 and M_2 . These configurations were then evolved in calculations where the eccentricity of the inner planet is damped on a constant timescale τ_e (while the semimajor axis of the inner planet is adjusted at the same time to conserve orbital angular momentum) to simulate tidal dissipation in the inner planet. We ignore tidal dissipation in the outer planet as the rate is a steep function of semimajor axis (Equation (12)). The results are plotted in Figures 3 and 4. In Figure 3 for 3:2, the dashed, solid, and dot-dashed lines are for $M_1 + M_2 = 20M_\oplus$ and $M_1/M_2 = 0.5, 1.0, \text{ and } 2.0$, respectively. In Figure 4 for 2:1, the dashed, solid, and dot-dashed lines are for $M_1 = M_2 = 5, 10, \text{ and } 20M_\oplus$, respectively. The figures show that

$$e_1 \propto (t/\tau_e)^{-1/3}, \quad (13)$$

and

$$\frac{P_2}{P_1} - \frac{j}{(j-1)} = (D_j t/\tau_e)^{1/3}, \quad (14)$$

after an initial transient period of a few τ_e . We have checked that the relationships in Equations (7) and (8) are satisfied during the power-law decay. Lithwick & Wu (2012), Batygin & Morbidelli (2013), and Delisle et al. (2012) have explained this power-law behavior (see also Papaloizou & Terquem 2010) and derived analytically D_j as a function of M_1/M_* and M_2/M_1 for the $j:(j-1)$ resonance:

$$D_j = \frac{9j^2}{(j-1)^3} \left(\frac{M_1}{M_*} \right)^2 \beta(1+\beta)C_1^2, \quad (15)$$

where

$$\beta = \frac{M_2}{M_1} \alpha^{-1/2} = \frac{M_2}{M_1} \left(\frac{j}{j-1} \right)^{1/3}. \quad (16)$$

The dotted lines in Figures 3 and 4 show the analytic result, which is in excellent agreement with the numerical results after the initial transient period.

We have so far assumed that tidal dissipation in the inner planet conserves the orbital angular momentum. Strictly speaking, tidal dissipation conserves the total angular momentum, which includes the spin angular momentum. There is a small change in D_j if we account for the tidal evolution of the planet’s spin. We have also ignored the tidal dissipation in the outer planet, which adds to D_j/τ_e but does not change the 1/3 power-law behavior (Lithwick & Wu 2012; Batygin & Morbidelli 2013).

An important consequence of this slow power-law behavior is that many τ_e must elapse to produce a departure of P_2/P_1 of a few percent from exact commensurability. For example, $P_2/P_1 - j/(j - 1) \approx 0.03$ requires $t \gtrsim 50\tau_e$ (see Figs. 3 and 4). For $P = 10$ days, $M_* = 1M_\odot$, $M_p = 10M_\oplus$, $R_p = 3R_\oplus$,

$$\tau_e = 2.26 \times 10^6 (Q/k_2) \text{ yr.} \quad (17)$$

Whether a near-resonance pair can reach its $P_2/P_1 - j/(j - 1)$ within the age of its host star (\sim a few Gyr) depends critically on Q/k_2 of the inner planet, which is very different for rocky and giant planets, as we now review.

3.1. Known Constraints on Q/k_2 of Planets

The tidal Q/k_2 of Solar System planets have been measured or constrained by the tidal evolution of their satellites. The known value and limit on Q/k_2 for rocky planets are $Q/k_2 = 40$ for Earth (Murray & Dermott 1999) and $470 < Q/k_2 < 1000$ for Mars (Shor 1975; Sinclair 1978; Duxbury & Callahan 1982). The known limits on Q/k_2 for giant planets are: $1.6 \times 10^5 < Q/k_2 < 5.3 \times 10^6$ for Jupiter (Yoder & Peale 1981), $5.4 \times 10^4 < Q/k_2 < 2.9 \times 10^5$ for Saturn (Peale 1999; Meyer & Wisdom 2008), $1.1 \times 10^5 < Q/k_2 < 3.8 \times 10^5$ for Uranus (Tittlemore & Wisdom 1990), and $2.2 \times 10^4 < Q/k_2 < 8.8 \times 10^4$ for Neptune (Banfield & Murray 1992; Zhang & Hamilton 2008). For extrasolar giant planets, $6.7 \times 10^4 < Q/k_2 < 6.7 \times 10^8$ has been derived from the existence of some close-in planets with non-zero orbital eccentricities (Matsumura et al. 2008). So the *lowest* bound on Q/k_2 is 40 for rocky planets from Earth and 2.2×10^4 for giant planets from Neptune.

If we substitute these lowest bounds into the estimate in Equation (17), we find $\tau_e \gtrsim 9 \times 10^7$ yr for rocky planets and $\tau_e \gtrsim 5 \times 10^{10}$ yr for giant planets, which indicate that a near-resonance pair might be able to reach its $P_2/P_1 - j/(j - 1)$ over the age of its host star, if the inner planet is rocky (and not if the inner planet is a giant).

4. COMPARISON WITH OBSERVATIONS

Figure 5 shows the tidal eccentricity damping timescale τ_e (Equation (12)) of the inner planet for the Kepler candidate pairs near the 2:1 and 3:2 resonances. Circles are adjacent pairs, and triangles are non-adjacent pairs. Filled and open symbols are pairs with the radius of the inner planet $R_1 < 2R_\oplus$ and $R_1 > 2R_\oplus$, respectively. For the “giant” planets with $R_p > 2R_\oplus$, we adopt $Q/k_2 = 10^5$ and mass from the mass-radius relationship $M_p = M_\oplus(R_p/R_\oplus)^{2.06}$ of Lissauer et al. (2011), which is consistent with Earth to Saturn in the Solar System (other proposed mass-radius relationships, such as those of Wu & Lithwick 2013 and Weiss et al. 2013, would give a similar plot). For the “rocky” planets with $R_p < 2R_\oplus$, we adopt $Q/k_2 = 100$ and mass from the mass-radius relationship $M_p = M_\oplus(R_p/R_\oplus)^{3.7}$ of Valencia et al. (2006). The dashed and solid lines in Figure 5 show τ_e as a function of P_2/P_1 according to equations (14) and (15) for $t = 1$ Gyr and 13.7 Gyr, respectively, if we have two $10M_\oplus$ planets orbiting a solar-mass star (i.e., $M_1/M_* = 3 \times 10^{-5}$ and $M_1 = M_2$). These lines indicate where such a resonant pair would be in P_2/P_1 , if it started near exact commensurability, its age is $t = 1$ Gyr or 13.7 Gyr, and the tidal eccentricity damping timescale of the inner planet is τ_e . There are some filled symbols below the solid lines for the age of the Universe, hinting that some of the near-resonance pairs with $R_1 < 2R_\oplus$ can potentially reach their current locations by tidal eccentricity damping in less than the age of the host star. Most of the pairs with $R_1 > 2R_\oplus$ (open symbols) are well above the lines, indicating that they are unlikely to reach their current locations by tidal eccentricity damping. However, the comparison in Figure 5 is not exact, as the theoretical curves are for a specific combination of stellar and planetary masses, and the observed Kepler pairs are plotted for assumed Q/k_2 .

Turning the inference around, we may assume that the current architecture was established by tides, and thereby infer constraints on Q/k_2 . We can plot (Equations (12) and (14))

$$\frac{Q}{k_2} = \frac{21\pi}{P_1} \frac{M_*}{M_1} \left(\frac{R_1}{a} \right)^5 [P_2/P_1 - j/(j-1)]^{-3} D_j t \quad (18)$$

versus P_2/P_1 near the $j:(j-1)$ resonance with $t = 13.7$ Gyr. This is the *maximum* Q/k_2 or minimum tidal dissipation efficiency that the inner planet must have if the pair is to evolve to its current P_2/P_1 in less than the age of the Universe. The actual Q/k_2 is smaller by the ratio of the age of the planetary system to the age of the Universe. In Figure 6, the points show this maximum Q/k_2 for the inner planet of the observed Kepler pairs. The four panels show the $R_1 < 2R_\oplus$ and $R_1 > 2R_\oplus$ cases for 3:2 and 2:1. The lines with arrows pointing upward are the known lowest bound on Q/k_2 for planets (2.2×10^4 for giant planets and 40 for rocky planets; see §3.1). Figure 6 clearly shows that some pairs with $R_1 < 2R_\oplus$ can reach where they are by tidal eccentricity damping, if planets with $R_p < 2R_\oplus$ are rocky with $Q/k_2 \geq 40$. They include KOI 500.03/04, KOI 500.04/01, KOI 730.02/01, KOI 961.01/03, and KOI 2038.01/02 just outside 3:2, and KOI 720.04/01, KOI 904.01/04, KOI 952.04/01, KOI 1161.03/01, and KOI 1824.02/01 just outside 2:1, which are ~ 20 – 33% of all pairs with $R_1 < 2R_\oplus$ in the period ratio ranges shown in Figure 6. However, none of the pairs with $R_1 > 2R_\oplus$ can reach their current P_2/P_1 , if planets

with $R_p > 2R_\oplus$ are giants with $Q/k_2 \geq 2.2 \times 10^4$. Furthermore, there are clumps of $R_1 > 2R_\oplus$ pairs just outside 2:1 and 3:2 that are more than an order of magnitude below $Q/k_2 = 2.2 \times 10^4$.

In Figure 6 we only plot the adjacent pairs, as the tidal evolution of the non-adjacent pairs can be significantly affected by secular or even resonant interactions with the intervening planet(s). Adjacent pairs with $R_1 > 2R_\oplus$ could evolve significantly faster, if the outer planet has $R_2 < 2R_\oplus$ and much lower Q/k_2 to overcome the steep dependence of the tidal eccentricity damping rate on orbital semimajor axis (Equation (12)). However, for the observed Kepler pairs with $R_1 > 2R_\oplus$ in the upper panels of Figure 6, only three with P_2/P_1 between 1.5 and 1.53 and two with P_2/P_1 between 2 and 2.06 have an outer planet with $R_2 < 2R_\oplus$. So our conclusion that most of the pairs with $R_1 > 2R_\oplus$ cannot reach their current P_2/P_1 by tidal eccentricity damping, if planets with $R_p > 2R_\oplus$ are giants with $Q/k_2 \geq 2.2 \times 10^4$, is robust.

In the above analysis, we follow the Kepler team in using $R_p = 2R_\oplus$ as the boundary between super-Earths and Neptunes. Some pairs are moved from the upper panels of Figure 6 to the lower panels if we increase this boundary to $R_p = 2.25R_\oplus$ (and vice versa if we decrease this boundary to $R_p = 1.75R_\oplus$), but the overall patterns (i.e., some pairs in the lower panels have maximum Q/k_2 of the inner planet above 40 and all pairs in the upper panels have maximum Q/k_2 of the inner planet below 2.2×10^4) remain the same.

5. SUMMARY AND DISCUSSION

We have shown that some of the Kepler near-resonance pairs with $R_1 < 2R_\oplus$ may be able to move to their current near-resonance locations by tidal damping of eccentricity if they are rocky with $Q/k_2 \sim 100$, but that all known pairs with $R_1 > 2R_\oplus$ are unable to move to their current near-resonance locations by the same mechanism if they are giants with $Q/k_2 \gtrsim 2 \times 10^4$.

What are the alternatives? One possibility is that some of the $R_p > 2R_\oplus$ planets are in fact rocky with low Q/k_2 . We have checked that increasing the boundary between super-Earths and Neptunes to, say, $R_p = 2.25R_\oplus$ does not change our conclusions. This possibility can also be checked by measuring or constraining the masses M_p , and hence the mean densities ρ_p , of the planets using transit timing variations (TTV) or radial velocity data. Wu & Lithwick (2013) have determined M_p and ρ_p for 16 pairs of Kepler planets from TTV (see also Lithwick et al. 2012; Xie 2012). Nine of these pairs are in the period ratio ranges plotted in Figure 6, all with $R_1 > 2R_\oplus$. Figure 7 shows the maximum Q/k_2 of the inner planet for these nine pairs according to Equation (18), with the open circles using assumed mass-radius relationships (same as in the upper panels of Figure 6) and the filled squares using the actual masses determined from TTV. The maximum Q/k_2 values shift when actual masses are used, but they remain more than an order of magnitude below the lowest bound $Q/k_2 = 2.2 \times 10^4$ for giant planets, and mostly above the lowest bound $Q/k_2 = 40$ for rocky planets. Although the inner planets of two pairs (KOI 1336.01/02 and KOI 168.03/01) have $\rho_p \geq 4.7 \text{ g cm}^{-3}$ that clearly exceed the bulk densities of uncompressed rocks, the inner planets of

three pairs (KOI 841.01/02, KOI 244.02/01, and KOI 248.01/02) have $\rho_p = 0.64\text{--}1.3 \text{ g cm}^{-3}$, which are more consistent with giant planets. Although Wu & Lithwick (2013) have suggested that the low densities of some planets with $R_p \leq 3R_\oplus$ (such as KOI 244.02 and KOI 248.01) could be due to an extended envelope of hydrogen and helium $\lesssim 1\%$ in mass on a rocky planet, KOI 841.01 (which has $R_p = 5.44R_\oplus$ and $\rho_p = 0.64 \text{ g cm}^{-3}$) is most likely a giant planet.

Another relevant case is the KOI 142 system, which has one transiting planetary candidate (KOI 142.01) that shows large TTV as well as detectable transit duration variations (TDV). Nesvorný et al. (2013) have determined from the TTV and TDV that KOI 142.01 has $R_p = 4.23_{-0.39}^{+0.30} R_\oplus$ and $\rho_p = 0.48_{-0.46}^{+0.54} \text{ g cm}^{-3}$ and that it is just wide of the 2:1 resonance ($P_2/P_1 = 2.03$) with an outer planet with $M_2 = 216M_\oplus$. Since there is also an estimated stellar age ($\approx 2.45 \text{ Gyr}$), we can determine from Equation (18) the actual (instead of maximum) Q/k_2 needed for KOI 142.01: 3400, which is lower than the lowest bound for giant planets by a factor of 6.5. However, this constraint on Q/k_2 of KOI 142.01 is unlikely to be valid, because the relatively large orbital eccentricities of both planets (mean $e_1 = 0.064$ and $e_2 = 0.055$) are not consistent with the tidal eccentricity damping scenario (Nesvorný et al. 2013).

So another mechanism is needed for some of the pairs with $R_1 > 2R_\oplus$. Petrovich et al. (2013) have considered the possibility of *in situ* formation of planets near first-order mean-motion resonances in a simple dynamical model without orbital migration or dissipation. For the effective viscosity and dimensionless scale height, H/a , typically assumed for protoplanetary disks, most of the Kepler candidates are sufficiently small that they are unable to open gaps in their natal protoplanetary disks and should undergo type I migration. Rein (2012) has suggested migration in a turbulent disk, which has both smooth and stochastic components, as a way to produce near-resonance pairs. The departure from exact commensurability can be used to constrain the relative strength of smooth and stochastic migration. However, Rein (2012) has assumed that the smooth migration is always inward, which is only true for classic type I (and type II) migration. Alternatively, Baruteau & Papaloizou (2013) have shown that planet-disk interactions for partial gap-opening planets may provide sufficient energy dissipation and eccentricity damping and lead to near-resonance pairs. However, effective viscosity and/or dimensionless scale height smaller than typical values is required for most of the Kepler candidates to open partial gaps.

Finally, we note that recent analysis of the corotation and horseshoe torques (plus the differential Lindblad torque) have shown that the coefficient C_a for the migration rate in Equation (9) is a function of the local surface density gradient $d \ln \Sigma / d \ln a$, temperature gradient $d \ln T / d \ln a$, viscous saturation parameter p_ν , and thermal saturation parameter p_χ (e.g., Paardekooper et al. 2010, 2011). In certain disk models (e.g., Garaud & Lin 2007), it is possible for type I migration to be outward in the viscously heated regions of the disk and in the region inside the magnetospheric truncation radius, if the corotation and horseshoe torques are not saturated (Paardekooper et al. 2011; Kretke & Lin 2012). There are also locations in the disk where the total torque vanishes and the migration is stalled. This more complex migration behavior means that it is possible for a pair of planets to undergo both convergent and divergent migration, as the disk accretion rate decreases

with time and the disk depletes. Whether the breaking of resonances by divergent migration could result in an excess of planet pairs just outside the first-order resonances will require further investigation. In this paper, however, we have shown that the later evolution due to tides is not enough to explain the structures near resonances.

We thank the referee for helpful comments on the manuscript. M.H.L. was supported by Hong Kong RGC grant HKU 7034/09P. D.F. was supported by NASA through Hubble Fellowship grant HF-51272.01-A awarded by STScI. D.N.C.L. was supported by NASA (NNX08AM84G), NSF (AST-0908807), and a University of California Lab Fee grant.

REFERENCES

- Artymowicz, P. 1993, *ApJ*, 419, 166
- Banfield, D., & Murray, N. 1992, *Icarus*, 99, 390
- Baruteau, C., & Papaloizou, J. C. B. 2013, *ApJ*, submitted (arXiv:1301.0779)
- Batalha, N. M., et al. 2013, *ApJS*, 204,24
- Batygin, K., & Morbidelli, A. 2013, *AJ*, 145, 1
- Bryden, G., Różyczka, M., Lin, D. N. C., & Bodenheimer, P. 2000, *ApJ*, 540, 1091
- Burke, C. J., et al. 2013, AAS Meeting, 221, 216.02
- Delisle, J.-B., Laskar, J., Correia, A. C. M., & Boué, G. 2012, *A&A*, 546, 71
- Duxbury, T. C., & Callahan, J. D. 1982, *Lunar Planet. Sci. Conf.*, 13, 191
- Fabrycky, D. C., et al. 2012, *ApJ*, submitted (arXiv:1202.6328)
- Garaud, P., & Lin, D. N. C. 2007, *ApJ*, 654, 606
- Goldreich, P., & Tremaine, S. 1980, *ApJ*, 241, 425
- Hut, P. 1981, *A&A*, 99, 126
- Kley, W. 2000, *MNRAS*, 313, L47
- Kretke, K. A., & Lin, D. N. C. 2012, *ApJ*, 755, 74
- Laughlin, G., & Chambers, J. E. 2001, *ApJ*, 551, L109
- Laughlin, G., Butler, R. P., Fischer, D. A., Marcy, G. W., Vogt, S. S., & Wolf, A. S. 2005, *ApJ*, 622, 1182

- Lee, M. H. 2004, *ApJ*, 611, 517
- Lee, M. H., & Peale, S. J. 2002, *ApJ*, 567, 596
- Lee, M. H., Butler, R. P., Fischer, D. A., Marcy, G. W., & Vogt S. S. 2006, *ApJ*, 641, 1178
- Lin, D. N. C., & Papaloizou, J. 1986, *ApJ*, 309, 846
- Lissauer, J. J., et al. 2011, *ApJS*, 197, 8
- Lissauer, J. J., et al. 2012, *ApJ*, 750, 112
- Lithwick, Y., & Wu, Y. 2012, *ApJ*, 756, L11
- Lithwick, Y., Xie, J., & Wu, Y. 2012, *ApJ*, 761, 122
- Matsumura, S., Genya, T., & Rasio, F. A. 2008, *ApJ*, 686, L29
- Meyer, J., & Wisdom, J. 2008, *Icarus*, 193, 178
- Murray, C. D., & Dermott, S. F. 1999, *Solar System Dynamics* (Cambridge: Cambridge Univ. Press)
- Nesvorný, D., Kipping, D., Terrell, D., Hartman, J., Bakos, G. A., & Buchhave, L. A. 2013, preprint (arXiv:1304.4283)
- Novak, G. S., Lai, D., & Lin, D. N. C. 2003, in *ASP Conf. Ser. 294, Scientific Frontiers in Research on Extrasolar Planets*, ed. D. Deming & S. Seager (San Francisco: ASP), 177
- Paardekooper, S.-J., Baruteau, C., Crida, A., & Kley, W. 2010, *MNRAS*, 401, 1950
- Paardekooper, S.-J., Baruteau, C., & Kley, W. 2011, *MNRAS*, 410, 293
- Papaloizou, J. C. B., & Terquem, C. 2010, *MNRAS*, 405, 573
- Peale, S. J. 1986, in *Satellites*, ed. J. A. Burns & M. S. Matthews (Tucson, Univ. Arizona Press), 159
- Peale, S. J. 1999, *ARA&A*, 37, 533
- Petrovich, C., Malhotra, R., & Tremaine, S. 2013, *ApJ*, 770, 24
- Rivera, E. J., & Lissauer, J. J. 2001, *ApJ*, 558, 392
- Rein, H. 2012, *MNRAS*, 427, L21
- Shor, V. A. 1975, *Celest. Mech.*, 12, 61
- Sinclair, A. T. 1978, *Vistas Astron.*, 22, 133

- Tan, X., Payne, M. J., Lee, M. H., Ford, E. B., Howard, A. W., Marcy, G. W., Johnson, J. A., & Wright J. T. 2013, ApJ, submitted (arXiv:1306.0687)
- Tanaka, H., Takeuchi, T., & Ward, W. R. 2002, ApJ, 565, 1257
- Tittemore, W. C., & Wisdom, J. 1990, Icarus, 85, 394
- Valencia, D., O’Connell, R. J., & Sasselov, D. 2006, Icarus, 181, 545
- Ward, W. R. 1997, Icarus, 126, 261
- Weiss, L. M., et al. 2013, ApJ, 768, 14
- Wu, Y., & Lithwick, Y. 2013, ApJ, in press (arXiv:1210.7810)
- Xie, J. 2012, ApJ, submitted (arXiv:1208.3312)
- Yoder, C. F., & Peale, S. J. 1981, Icarus, 47, 1
- Zhang, K., & Hamilton, D. P. 2008, Icarus, 193, 267

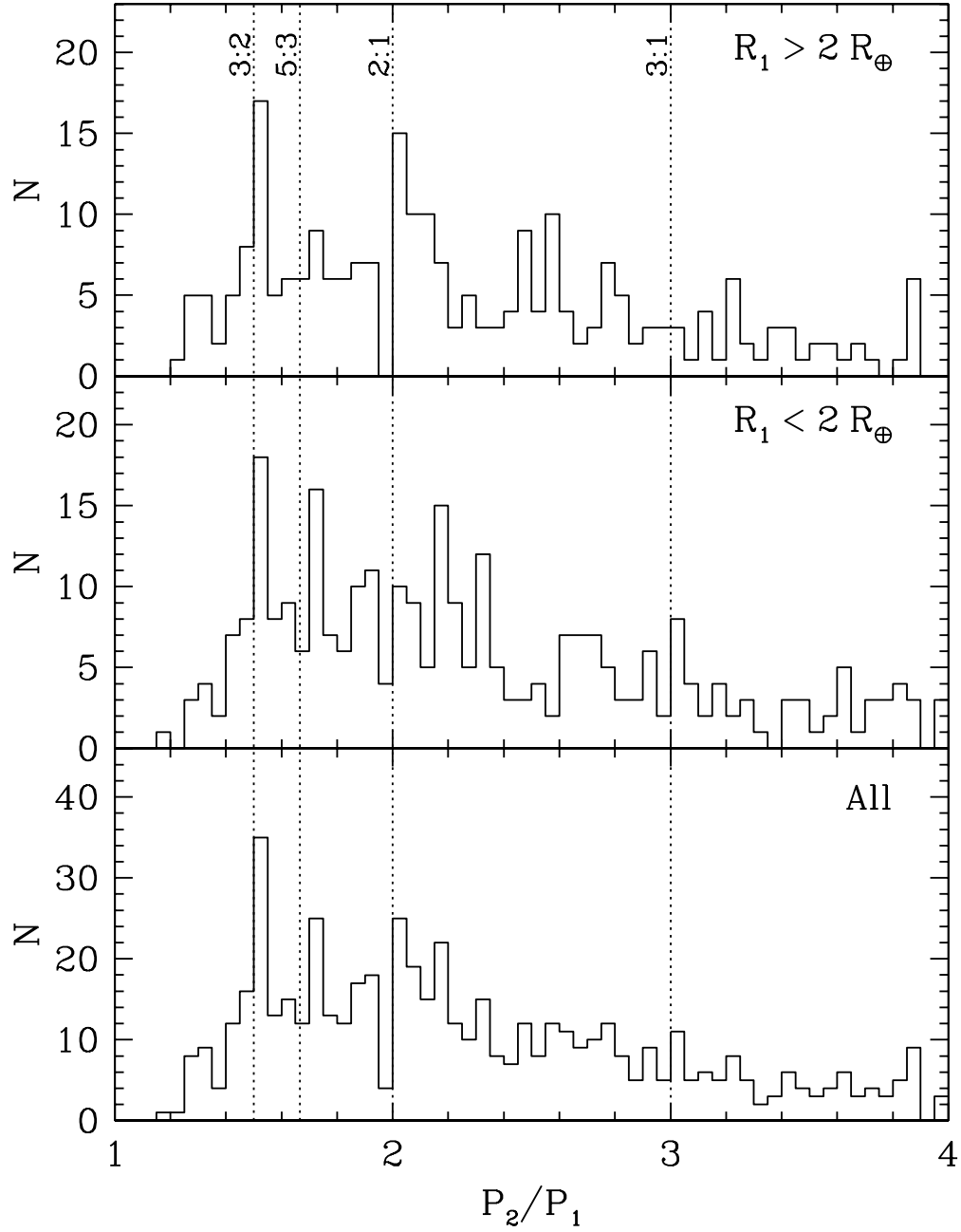


Fig. 1.— Histogram of period ratio P_2/P_1 for all Kepler candidate pairs (bottom panel), pairs with radius of the inner planet $R_1 < 2R_\oplus$ (middle panel), and pairs with $R_1 > 2R_\oplus$ (upper panel). The dotted lines mark the exact period commensurabilities for the 3:1, 2:1, 5:3 and 3:2 resonances.

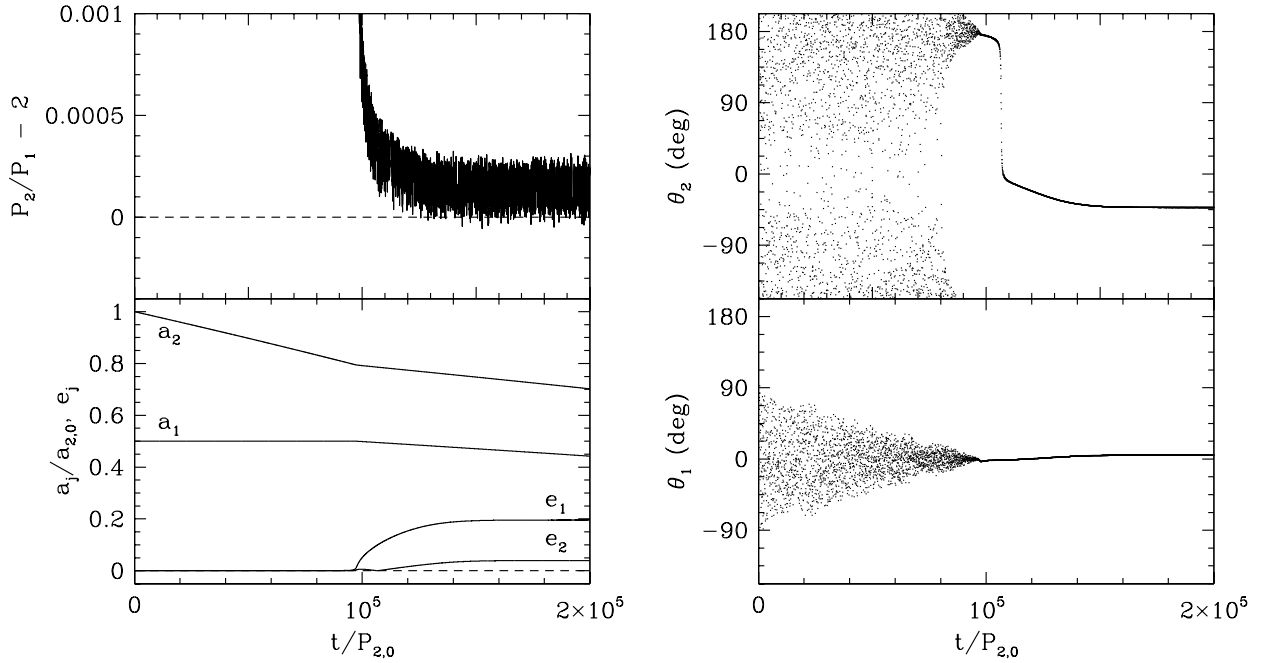


Fig. 2.— Evolution of the semimajor axes a_1 and a_2 , eccentricities e_1 and e_2 , departure of the period ratio P_2/P_1 from 2, and 2:1 eccentricity-type resonance variables $\theta_1 = \lambda_1 - 2\lambda_2 + \varpi_1$ and $\theta_2 = \lambda_1 - 2\lambda_2 + \varpi_2$, for a convergent migration calculation with the stellar mass $M_* = 1M_\odot$ and planetary masses $M_1 = M_2 = 10M_\oplus$. The outer planet is forced to migrate inward with $\dot{a}_2/a_2 = -2 \times 10^{-6}/P_2$ and eccentricity damping factor $K_e = 100$. The semimajor axes and time are in units of the initial orbital semimajor axis, $a_{2,0}$, and period, $P_{2,0}$, of the outer planet, respectively.

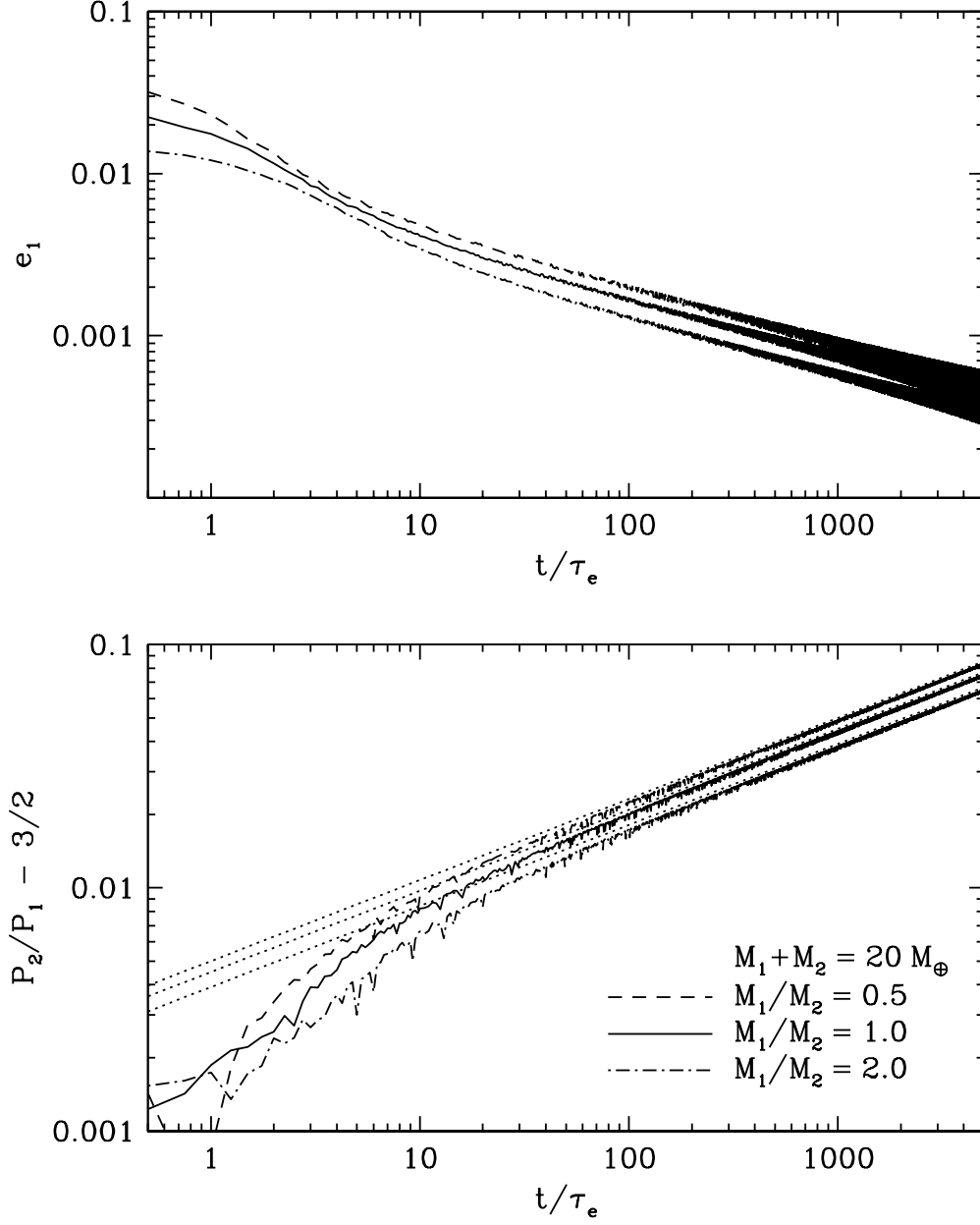


Fig. 3.— Evolution of the departure of the period ratio P_2/P_1 from 3/2 and eccentricity of the inner planet e_1 for numerical calculations where e_1 is damped on a constant timescale τ_e to simulate tidal dissipation in the inner planet. The planet pair is initially in the 3:2 resonance, with $M_* = 1M_\odot$, $M_1 + M_2 = 20M_\oplus$, and $M_1/M_2 = 0.5$ (dashed lines), 1.0 (solid lines), and 2.0 (dot-dashed lines). The dotted lines in the lower panel show Equations (14) and (15) from the analytic theory.

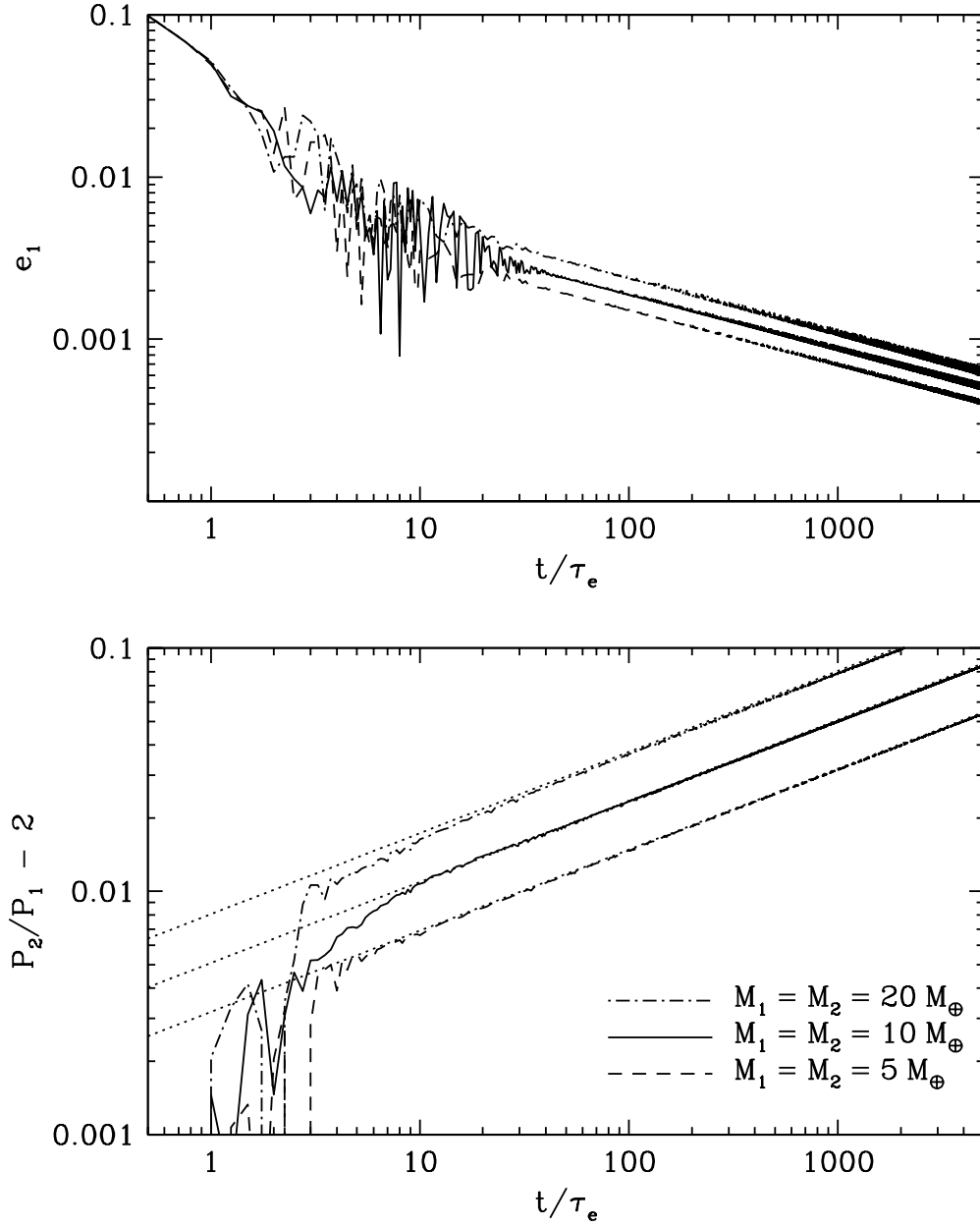


Fig. 4.— Same as Figure 3, but for the 2:1 resonance with $M_1 = M_2 = 5M_\oplus$ (dashed lines), $10M_\oplus$ (solid lines), and $20M_\oplus$ (dot-dashed lines).

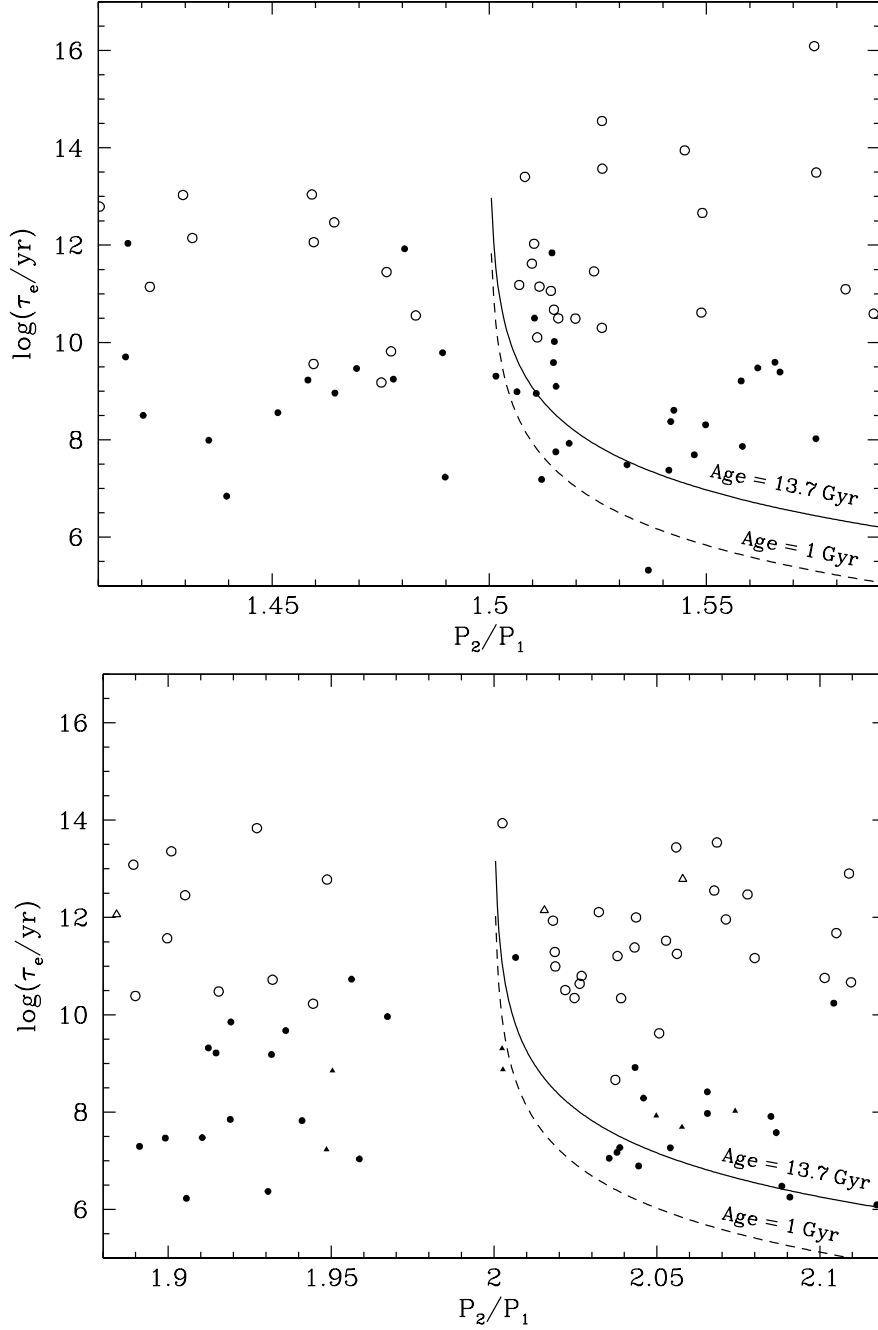


Fig. 5.— Tidal eccentricity damping timescale τ_e (Equation (12)) of the inner planet for the Kepler candidate pairs near the 2:1 (lower panel) and 3:2 (upper panel) resonances. Circles and triangles are adjacent and non-adjacent pairs, respectively, and filled and open symbols are pairs with $R_1 < 2R_\oplus$ and $R_1 > 2R_\oplus$, respectively. We adopt $Q/k_2 = 10^5$ and $M_p = M_\oplus (R_p/R_\oplus)^{2.06}$ for planets with $R_p > 2R_\oplus$, and $Q/k_2 = 100$ and $M_p = M_\oplus (R_p/R_\oplus)^{3.7}$ for planets with $R_p < 2R_\oplus$. The dashed and solid lines show τ_e as a function of P_2/P_1 according to Equations (14) and (15) for $t = 1$ and 13.7 Gyr, respectively, if we have two $10M_\oplus$ planets orbiting a solar-mass star.

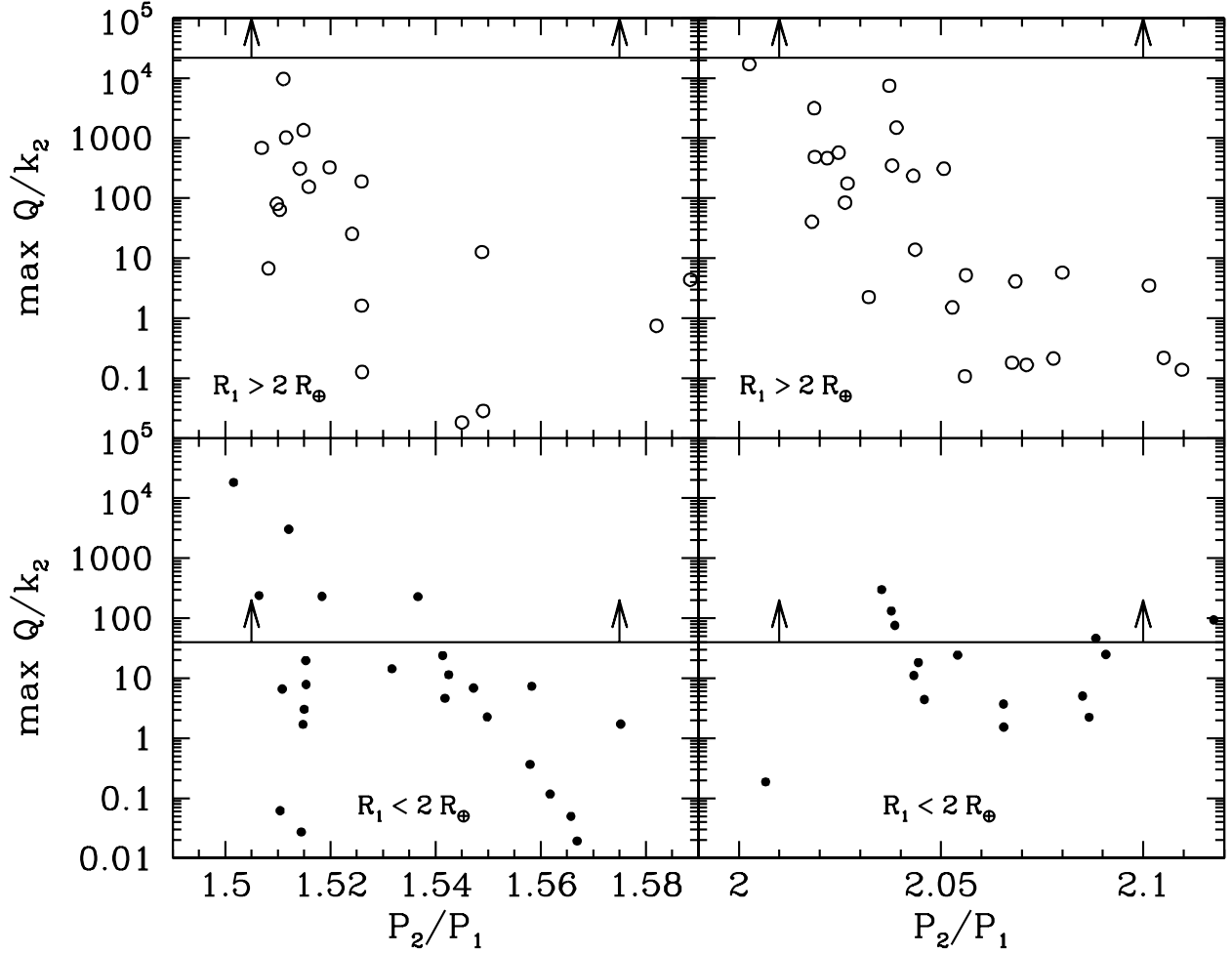


Fig. 6.— Maximum Q/k_2 (Equation (18)) that the inner planet must have if the Kepler near-resonance pairs are to evolve to their current P_2/P_1 in less than 13.7 Gyr. The pairs with $R_1 < 2R_\oplus$ (lower panels) and $R_1 > 2R_\oplus$ (upper panels) are shown in the left and right panels for the 3:2 and 2:1 resonances, respectively. We adopt $M_p = M_\oplus(R_p/R_\oplus)^{2.06}$ for planets with $R_p > 2R_\oplus$, and $Q/k_2 = 100$ and $M_p = M_\oplus(R_p/R_\oplus)^{3.7}$ for planets with $R_p < 2R_\oplus$. The lines with arrows pointing upward are the known lowest bound on Q/k_2 : 2.2×10^4 for giant planets and 40 for rocky planets.

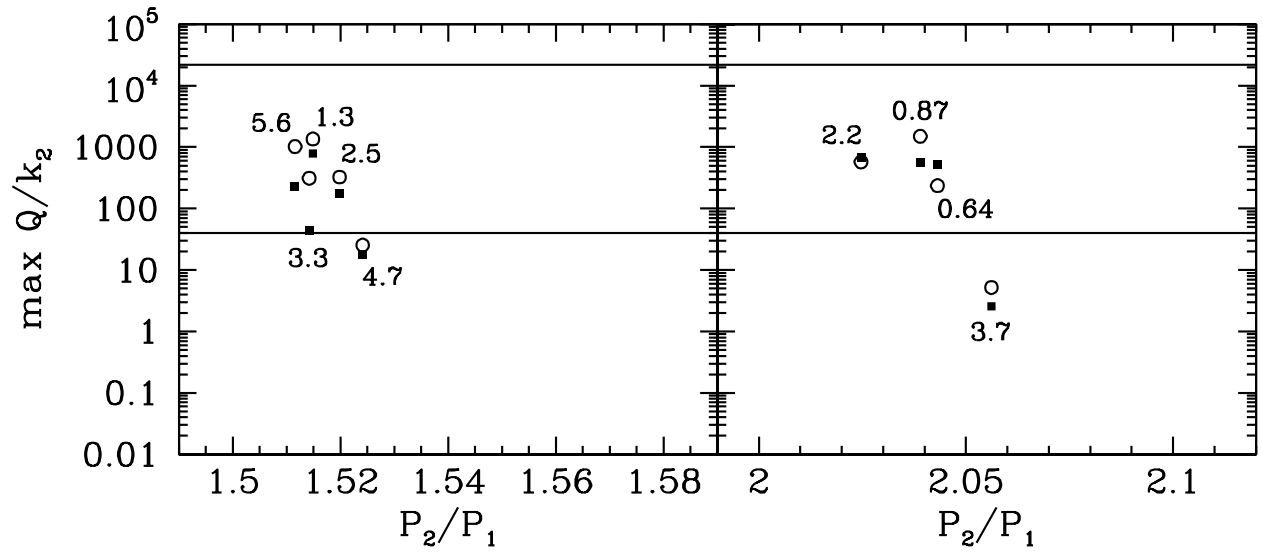


Fig. 7.— Same as Figure 6, but for the pairs with planetary masses obtained from transit timing variations (TTV) by Wu & Lithwick (2013). All pairs in this sample have $R_1 > 2R_\oplus$. Each pair shifts vertically from the maximum Q/k_2 determined using assumed mass-radius relationships (open circle; same as in the upper panels of Figure 6) to that using the actual masses from TTV (filled square). The numerical value next to each pair indicates the mean density (in g cm^{-3}) of the inner planet from TTV.